

NJC

Accepted Manuscript



This is an *Accepted Manuscript*, which has been through the Royal Society of Chemistry peer review process and has been accepted for publication.

Accepted Manuscripts are published online shortly after acceptance, before technical editing, formatting and proof reading. Using this free service, authors can make their results available to the community, in citable form, before we publish the edited article. We will replace this *Accepted Manuscript* with the edited and formatted *Advance Article* as soon as it is available.

You can find more information about *Accepted Manuscripts* in the [Information for Authors](#).

Please note that technical editing may introduce minor changes to the text and/or graphics, which may alter content. The journal's standard [Terms & Conditions](#) and the [Ethical guidelines](#) still apply. In no event shall the Royal Society of Chemistry be held responsible for any errors or omissions in this *Accepted Manuscript* or any consequences arising from the use of any information it contains.



Journal Name

ARTICLE

Hydrothermal formation of graphene aerogel for oil sorption: the role of reducing agent, reaction time and temperature†

Wenchao Wan,^{a,b} Fei Zhang,^b Shan Yu,^b Ruiyang Zhang,^b and Ying Zhou^{a,b*}

††Received 00th January 20xx,
Accepted 00th January 20xx

DOI: 10.1039/x0xx00000x

www.rsc.org/

Graphene aerogel (GA) is widely studied in oil contamination field in recent years. Among the preparation approaches, the hydrothermal treatment employing a certain reducing agent has attracted much attentions owing to the environmentally friendly and facile synthesis process. In this work, we systematically investigate the effects of various reducing agents including ammonia, ethanediamine (EDA) and vitamin C (VC) at different hydrothermal temperature (80, 100, 120, 140, 160, 180 °C) and reaction time (4, 8, 12, 16, 20, 24 h) on the density, specific surface area (SSA), strength, morphology and adsorption performance of GA. The results reveal that GA reduced by VC possesses the most outstanding performance on mechanical strength and re-utilization but has poor adsorption capacity (Q_{wt}), whereas the sample obtained with ammonia exhibits the highest Q_{wt} for both lube (160 g g⁻¹) and n-hexane (105 g g⁻¹). However, this sample not only reveals the worst mechanical strength which lead to a sharp decreasing of Q_{wt} during the adsorption-squeezing experiments, but the GA reduced by ammonia is also very sensitive to the reaction time and temperature. Therefore, EDA is a very promising reducing agent for hydrothermal process as the resulted GA can maintain the high Q_{wt} and reveal a wide hydrothermal preparation window.

1. Introduction

With the development of economy, the pollution coming from the oil industry has attracted worldwide attention.^{1a} Especially, the frequent occurrence of oil spill has caused immeasurable loss for our modern society. For instance, the deepwater horizon oil spill incident has lead to over 5000000 barrels of crude oil emitting into the Gulf of Mexico, which resulted in grave threats to the marine ecosystems and human health.^{1b} Among the methods for oil remediation, the use of adsorbing materials has been considered as one of the most efficient and inexpensive strategies. Nevertheless, the traditional adsorbents often suffered from low adsorption capacity, poor selectivity and secondary pollution. Generally, materials used for oil sorption should meet the demands including low density, highly adsorption efficiency, facile fabrication as well as repeated use. Therefore, graphene-based 3D porous macrostructure materials are deemed to be one of the most desirable selection.² Graphene aerogel (GA) possessing low density, high porosity, super-elasticity and high specific surface area has attracted increasing attentions over past years to address oil contamination.² Recently, 3D GA has been successfully prepared by various routes such as template directed chemical vapor deposition (CVD),³ pyrolyzation⁴ and fluid assembly of graphene oxide (GO) by hydrothermal treatment.² CVD is a sophisticated synthesis route and involves the use of expensive facilities, which limits the massive fabrication. In addition, although the pyrolyzation of carbon-rich precursors has been widely used for the preparation of GA, the high energy consumption and poor mechanical strength are obvious drawbacks for oil remediation applications.⁴ Compared to these two methods, hydrothermal technique is very prominent which offers

many advantages such as mild condition and tunable reaction parameters to prepare GA with excellent mechanical strength, low density, super-elasticity and re-utilization.⁵

In a typical hydrothermal process, GO is usually used as precursor due to its excellent hydrophilicity and well dispersion in water.⁶ Under hydrothermal treatment condition, the reduction agents can remove most of the oxygenic functional groups on the GO and extract the hydrophobic graphene from the GO solution to assemble into the designated size and shape depending on the reactor.⁷ Hence, the GA prepared through different reducing agents exhibits apparently distinct properties. Previously, various reducing agents including metal ions (Fe²⁺), N₂H₄, NaBH₄, ammonia, EDA and VC have been employed.^{8,9} For instance, GA reduced by metal ions can reveal multifunctional properties such as magnetic and photocatalysis, but exhibits a much higher density which significantly decreases the adsorption capacity.¹⁰ Duong and Yan et al. have investigated the influences of various reducing agents including VC, Na₂S, HI and NaHSO₃ on the morphology and electrical conductivity of GA.^{11,12} Furthermore, the influences of reaction time have also been studied by Xu et al.⁷ Yet, most of the previous work only studied parts of the reaction conditions and focused on the electrical properties. To the best of our knowledge, little work has systematically reported the effects of hydrothermal reaction conditions on the oil sorption properties.

Herein, we report the effects of environmental friendly reducing agents including EDA, VC and ammonia on the morphology, microstructure as well as oil sorption properties (adsorption capacity and reusability). In addition, the influences of temperature and reaction time were investigated systematically as well. Our current study points out the important role of hydrothermal treatment parameters on the oil remediation.

2. Experimental

2.1 Materials

Graphite powders (average lateral size of 500 μm) were purchased from Qingdao Jin Ri Lai Graphite Co., Ltd. EDA, H_2SO_4 (98 wt.%), KMnO_4 , P_2O_5 , H_2O_2 (30 wt.%), $\text{K}_2\text{S}_2\text{O}_8$ and $\text{C}_2\text{H}_5\text{OH}$ were purchased from Chengdu Kelong Chemical Co., Ltd. High-purity milli-Q water was used in all experiments.

2.2 Preparation of GO and GA

GO was prepared according to the previous work.^{13,14} In a typical procedure, 5 g of natural graphite flakes were added gradually into a 1:3 (volume ratio) mixture of fuming nitric acid and sulfuric acid (200 mL). The mixture was stirred at room temperature for 24 h under the magnetic stirring. After that, the mixture was diluted with water and the solids were collected through filtration. The obtained solid products were washed several times with water and dried at 60 $^\circ\text{C}$. Then, the dried powders were transferred into an oven at 1000 $^\circ\text{C}$ for ca. 10 s to make the graphite inflatable. After that, 5 g of powders, 300 mL of sulfuric acid, 4.2 g $\text{K}_2\text{S}_2\text{O}_8$ and 6.2 g P_2O_5 were successively added into a flask at 80 $^\circ\text{C}$ for 5 h under the magnetic stirring. After cooling to ambient temperature, the UP water was poured into the mixture. The suspension was filtered and washed with water using a 0.22 μm pore polycarbonate membrane. The obtained products were dried in air at room temperature. Then, the solids were added into 200 mL concentrated H_2SO_4 at 0 $^\circ\text{C}$ and 15 g KMnO_4 was added slowly (ca. 1 h) under continuous magnetic stirring condition. The mixture was heated to 35 $^\circ\text{C}$ for 2 h. After that, the mixture was diluted with 2 L of water, followed through the addition of 10 mL H_2O_2 . The mixture was deposited for 2 days and then the upper clarified liquid was removed. The precipitates were washed with water and 1 M HCl. Finally, the washed GO solution was calibrated to 2 mg/mL for further experiments. For the GA preparation, 160 μL reducing agents (VC, EDA and ammonia) with the mass percentage of 25% were added gradually into 40 mL GO solution under magnetic stirring. After 30 min, the mixed solution was transferred into a Teflon-lined stainless steel autoclave and heated at different temperatures for certain time to prepare graphene hydrogel. The obtained hydrogel was washed with water and freeze-dried (-80 $^\circ\text{C}$ pre-cooling) to prepare GA.

2.3 Characterizations

The powder X-ray diffraction (PXRD) patterns were performed through a PANalytical X'pert diffractometer operated at 40 kV and 40 mA using $\text{Cu K}\alpha$ radiation. The Raman spectra of these samples were analyzed on a micro-Raman 2000 system. Scanning electron microscopy (SEM) was measured on a Hitachi S-4800 microscope. The contact angles of water over these samples were tested on a JGW-360A. The Fourier transform infrared (FT-IR) spectra were recorded on a Nicolet 6700 spectrometer. The elemental analysis was detected on the Var10EL-3 elemental analyzer. The specific surface area (SSA) was determined through the adsorption of methylene blue (MB) adsorption method by UV-vis absorption spectrometer (UV-5100, Anhui Wanyi),¹⁵ which was calculated using the following equation:

$$\text{SSA} = \frac{N_A A_{\text{MB}} (C_0 - C_e) V}{M_{\text{MB}} m_s}$$

where N_A is Avogadro number ($6.02 \times 10^{23} \text{ mol}^{-1}$), A_{MB} is the covered area of per MB molecule (typically assumed to be 1.35 nm^2), C_0 and C_e are the initial and equilibrium concentrations of MB, respectively, V is the volume of MB solution, M_{MB} is the relative molecular mass of MB, and m_s is the mass of the sample.

2.4 Adsorption capacity measurements

For the oil-water adsorption experiments, toluene was stained with Sudan red. Then, 2 mL of the stained toluene was added to water and 5.8 mg of the obtained graphene aerogels (GAs) was immersed into this solution. The adsorbents were removed after the complete adsorption. Oil (lube) and n-hexane were selected to investigate the adsorption performances of the prepared GAs. Firstly, the weight of the GA adsorbents was recorded before immersing in the target adsorbate. Then, the adsorbent was weighed again after 5 min of immersing. The adsorption capacity (Q_{wt}) is the ratio of the final weight (m_1) after full adsorption to the initial weight (m_0) of GA as follows:

$$Q_{\text{wt}} = \frac{m_1 - m_0}{m_0}$$

The adsorption-squeezing experiments were carried out through the following steps: n-hexane was dropped on the surface of the aerogels until the adsorbent reached adsorption saturation and then the aerogels were squeezed to half of its height. The same process was repeated for 10 times, which is similar to our previous work.¹³

3. Results and Discussion

3.1 The effects of reducing agents

First of all, we fixed the temperature at 120 $^\circ\text{C}$ with 6 h of reaction time to investigate the role of reducing agent on the basis of our previous reaction conditions.¹³ Fig.1a shows the PXRD patterns of graphite, GO and GAs reduced by ammonia, EDA and VC. It was observed a strong diffraction peak at $2\theta=26.3^\circ$ (d-spacing = 3.4 \AA) for graphite and a sharp diffraction peak at $2\theta = 9.9^\circ$ (d-spacing = 8.9 \AA) for GO, whereas the diffraction peak of GAs reduced by different reducing agents (Ammonia, EDA and VC) are 25.1 $^\circ$ (d-spacing = 3.5 \AA), 24.3 $^\circ$ (d-spacing = 3.6 \AA) and 25.5 $^\circ$ (d-spacing = 3.5 \AA), respectively. Obviously, the interlayer spacing of the obtained GAs is much smaller than that of GO precursor but is slightly larger than that of the natural graphite. These results reveal the existence of π - π stacking between graphene sheets which are the characteristic structures of graphite and indicate the residual oxygen containing functional groups left on the reduced GO sheets. In addition, the broad diffraction peak of GAs also demonstrates the distribution of disordered graphene sheets and residual damaged structures in the reduced GO,¹¹⁻¹⁴ which are further confirmed by

Raman spectra. Two characteristic bands at 1355 cm^{-1} and 1590 cm^{-1} corresponding to the D and G bands were observed for all the measured samples (Fig. 1b). These bands represent the defects and disorders in the graphite like materials. The intensity ratio of D and G bands (I_D/I_G) of the GAs reduced by ammonia (1.12), EDA (1.13) and VC (1.15) is significantly larger than that of GO precursor (1.02), indicating the disordered graphene sheets and defective structures have been improved for the obtained GAs.^{15a, 16}

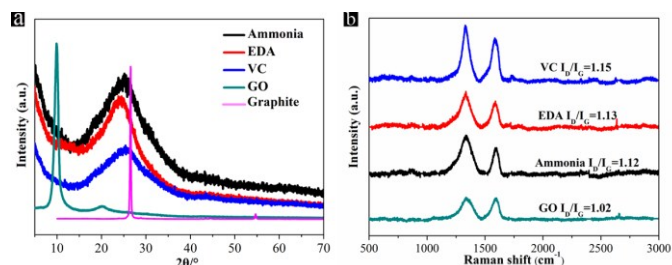


Fig. 1 (a) PXRD patterns of graphite, GO and GAs reduced by ammonia, EDA and VC; (b) Raman spectra of GO and GA reduced by ammonia, EDA and VC at $120\text{ }^{\circ}\text{C}$ for 6 h.

To understand the influences of functional groups of the reducing agents, FT-IR spectra of the obtained GAs were measured as shown in Fig. 2. The typical functional groups of the GO such as C-O at 1100 cm^{-1} , C=O stretching of the carbonyl (COOH) at 1640 cm^{-1} , C-C at the 1650 cm^{-1} and -OH at the 3400 cm^{-1} were observed for all the samples. Nevertheless, the peak of C-O in these samples is obviously distinguished with each other in terms of peak intensity and area, which reflects the reduction degree of the GO precursor. On the basis of these results, we can draw a conclusion that VC possesses the strongest reduction ability over the other two reducing agents, which is coincided with the reduction sequence of the three reducing agents: VC > EDA > ammonia. Moreover, C=N and N-H at ca. 2300 and 3000 cm^{-1} were observed for the samples reduced by ammonia and EDA, indicating that the functional groups of the reducing agents can be residual in the final products. This can be also confirmed from elemental analysis (Table. S1). In line with the FT-IR spectra results (Fig. 2), the elements of the reducing agents remain in the GAs. For example, significant amount of N from the EDA (8.79%) and ammonia (8.48%) were detected in the corresponding GAs, whereas tiny amount of N (0.52 wt.%) found in the GA (reduced by VC) as well as the S element should be from the preparation of GO. The previous work have demonstrated that the residual functional groups from precursor can deeply affect the properties such as the electrical conductivity and thermal stability of GA.^{8d, 11, 12} We expect that the residual functional groups could also affect the morphology, mechanical strength as well as adsorption capacity, which will be studied in the following parts.

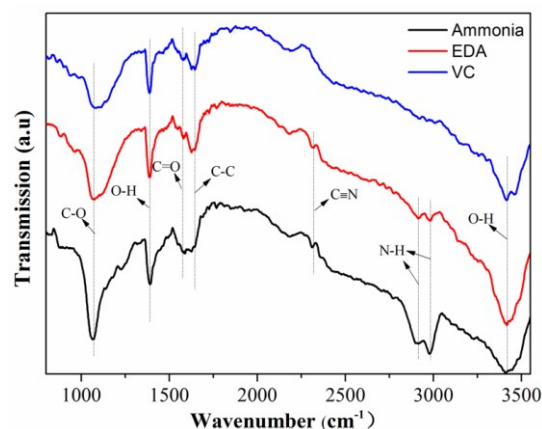


Fig. 2 FT-IR spectra of the GAs prepared with the Ammonia, EDA and VC at $120\text{ }^{\circ}\text{C}$ for 6 h.

Typical SEM images of the GAs reduced by VC, EDA and ammonia are shown in Fig. 3a-c. 3D networks are clearly observed for all the GA samples. Nevertheless, the pore sizes of GA reduced by ammonia are more uniform and the pore walls consisting of graphene sheets are thinner than that of the GAs reduced by EDA and VC. Among these samples, the GA reduced by VC aggregated very severely (Fig. 3a). The pore walls consisting of graphene sheets are markedly dense and the surface is occupied by some small graphene fragments which could be attributed to the reduction ability of the reducing agent as well as the role of the residual functional groups remained from the precursors. In a typical hydrothermal process, the hydrophobic graphene sheets are gradually restored out from the GO solution and assemble into hydrogel.⁷ The reducing agents in the solution can accelerate this process. Hence, the strong reducing agents VC, acted the role of accelerator, can greatly promote the agglomeration process. This is also reflected from the macroscopic photographs (Fig. 3d-f). In line with the morphology observation, GA reduced by VC reveals the smallest size and compacts densely, whereas the GAs prepared by EDA and ammonia are flexible. It is worth noting that all of these GAs are obtained from the equal amount of GO solution. Fig. 3g-i show the water contact angles of the prepared GAs. Among these samples, GA reduced by VC exhibits the highest water contact angle of 131.4° , whereas the other two GAs show the contact angle as low as 73.4° (EDA) and 78.2° (ammonia), which could be attributed to the left hydrophilic functional groups from reducing agents such as N-H (Fig. 2). Moreover, the surface morphology could also affect the hydrophobicity of the GA.^{17a} GA reduced with VC possesses a coarse surface which leads to a higher hydrophobicity, while GAs reduced with EDA and ammonia reveal smooth and metal-like surface. Considering the excellent hydrophobicity of the GA reduced by VC, the oil-water separation experiment was performed. As shown in Fig. S1, toluene was immediately adsorbed. The completely selective adsorption process only took 30 s. In addition, these GAs exhibit different densities (Table 1): the GA reduced with VC is 13.7 mg/cm^3 , while the samples reduced by ammonia and EDA are 4.9 and 6.8 mg/cm^3 , respectively. Furthermore, SSA of these GA samples was determined through the MB adsorption method (Table 1). The GA reduced by ammonia possessed much higher SSA (1089

g/m^2) than that of the sample reduced by VC ($661 \text{ g}/\text{m}^2$) and EDA ($440 \text{ g}/\text{m}^2$). The SSA of the GA reduced with VC is relatively high compared to that of the sample reduced by EDA. This could be because the GA reduced with VC possesses a wide distribution of pore size^{17b,18} and the nano-sized pores are unlikely to be enwrapped by the macromolecular organics. Furthermore, the pH values of these three kinds of mixed solution before transferring into the autoclave were monitored. The results reveal that the pH of the solution containing VC is 3.4, while the solution with ammonia and EDA is 11 and 10.4. Therefore, the distinct surface roughness could associate with the different pH values which are determined by the functional groups of the reducing agents. Previous reports have proved that the alkaline environment is facile to acquire the graphene sheets with large size and thin morphology, whereas the acid condition can accelerate the agglomeration and fragmentation of the graphene sheets.^{17,18}

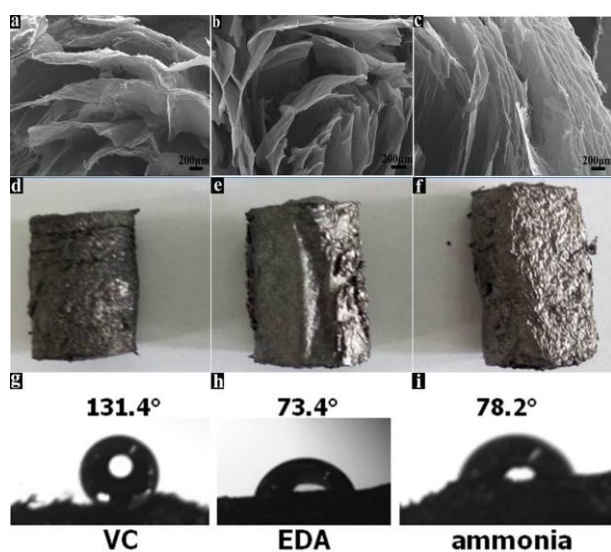


Fig. 3 Typical SEM images and contact angles of the GAs prepared by various reducing agents at 120°C for 6h (a) VC; (b) EDA; (c) ammonia and their corresponding Photographs (d) VC; (e) EDA; (f) ammonia; the water contact angles of GAs reduced by (g) VC, (h) EDA and (i) ammonia.

To investigate the adsorption properties of these GA samples, two kinds of common organics with different densities including lube ($0.910 \text{ g}/\text{cm}^3$) and n-hexane ($0.692 \text{ g}/\text{cm}^3$) were selected for the evaluation experiments. As shown in Fig. 4b and Table 1, the GA reduced by ammonia exhibits the highest adsorption capacity (Q_{wt}) for both lube (160 g g^{-1}) and n-hexane (105 g g^{-1}), while the sample reduced by VC reveals the lowest adsorption performances, which could be mainly attributed to the stronger reducibility of VC resulting in a severer agglomeration of the graphene. This phenomenon has been clearly demonstrated by the SEM observation, density and SSA measurements (Fig. 3 and Table 1). Furthermore, the Q_{wt} of the prepared GAs depends on the density of the target adsorbates. The Q_{wt} increases with the increasing of the density of the adsorbates for all the samples. Generally, the adsorption volume of organics is certain, thus the low density of the organics inevitably leads to a decreasing of adsorption capacity. Moreover, we selected chloroform with a larger density than water

to perform oil-water separation experiments (Table S2). The results are shown in Movie S1-S3 and Fig. S2 corresponding to using VC, EDA and ammonia as reducing agents. Although the GAs reduced by EDA and ammonia have a poor hydrophobicity, both of them show good adsorption abilities for the chloroform in the water. Considering the viscosity of lube is larger than that of water (Table S2), we could conclude that the obtained GAs can adsorb the oil with larger viscosity or density than water.

Table 1 Adsorption capacity, density, specific surface area of the GAs reduced with various reducing agents. The $Q_{\text{wt-10}}$ means the adsorption after ten times of squeezing.

GA samples	Density mg/cm^3	SSA m^2/g	Q_{wt} lube	Q_{wt} n-hexane	$Q_{\text{wt-10}}$ n-hexane
VC	13.7	661	88	58	49
EDA	6.8	440	140	98	75
Ammonia	4.9	1089	160	105	66

The reutilization of aerogels is very important for practical oil remediation applications. Firstly, we test the mechanical strength of these three GAs with a 50 g counterweight (Fig. 4a). The results indicate that the GA prepared by VC possesses the highest mechanical strength. Subsequently, the adsorption-squeezing experiments were performed and n-hexane was selected as the target adsorbate. The detailed procedure was shown in the Movie S4 and Movie S5. Obviously, the GA reduced by VC exhibited much better mechanical strength than that of the sample reduced by ammonia as this sample cannot return to their original height after squeezing to half of its height. Furthermore, Fig. 4c-e show the adsorption-squeezing experimental results, where the ordinate and abscissa represent the adsorption capacity and the cycle times, respectively. It was observed that the Q_{wt} of all the samples decreased in certain degree after ten cycling times. However, the decreasing of the GA reduced with ammonia is much more severe with the percentage of 38%, whereas the EDA is about 21%. The GA reduced with VC reveals the most stable performance and the Q_{wt} is only decreased ca.16%. In addition, for the use VC as a reducing agent, the Q_{wt} decreased only in the first cycle and the subsequent decrease is negligible. Different from the VC, the Q_{wt} of the GAs reduced by ammonia and EDA decreased almost in every cycle. Fig. S3 shows the photographs of these GAs before and after adsorption-squeezing experiments. Only the sample reduced by VC can maintain its original shape which is in line with the cycling performances. Generally, VC as the strongest reducer can promote the recovery of the structure and the π - π stacking between recovered graphene sheets also can firm the whole structure of the GA. On the other hand, the agglomeration and fragmentation on the graphene sheets promoted by the acid functional groups result in a higher density of GA, which can also enhance the mechanical strength. All in all, the application of GA in oil remediation is a complex interplay among surface property, density, mechanical strength, SSA, morphology and so on, which require the systematic optimization of preparation conditions. For example, the sample reduced by ammonia exhibits the best adsorption capacity (160 g g^{-1} for lube and 105 g g^{-1} for n-hexane) but reveals the worst

mechanical strength which lead to a sharp decreasing of Q_{wt} during adsorption-squeezing experiments (Fig. 4e).

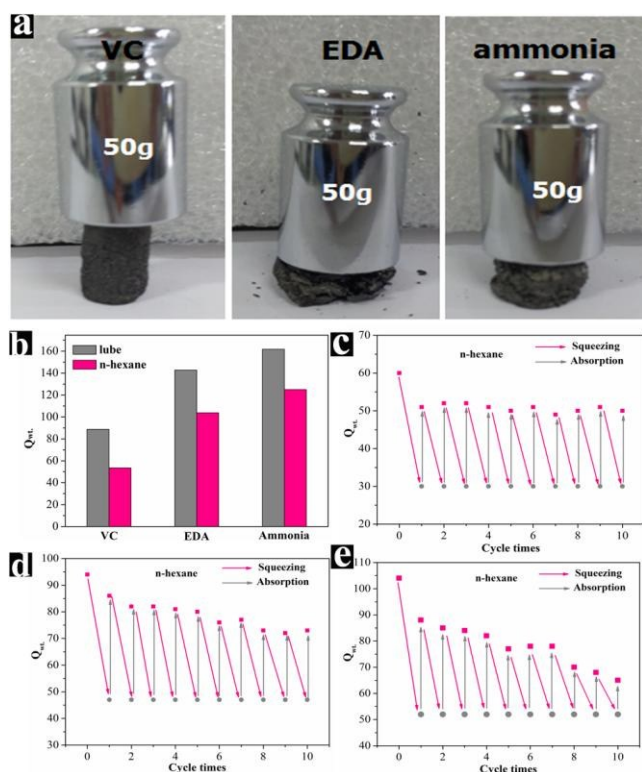


Fig. 4 (a) The mechanical strength of the prepared GAs; (b) the adsorption capacity of the obtained GAs; adsorption-squeezing experiments of the samples reduced by (c) VC, (d) EDA and (e) ammonia

3.2 The effects of reaction time

According to the above investigations, the GA reduced by ammonia reveals the highest Q_{wt} . However, other properties such as reutilization and mechanical strength are unsatisfactory, which consequently restricted its application in oil remediation. Therefore, the hydrothermal reaction condition needs to be further optimized. The temperature was fixed at 120 °C and the effects of reaction time were studied. Fig. 5 compared the SEM images of the GAs reduced by ammonia and EDA with different reaction time. Using ammonia as reducing agent, the graphene sheets in the GA are not interconnected very tightly and the graphene sheets disperse independently at the reaction time of 4 h (Fig. 5a). Hence, such short time is unable to form a firm interaction between graphene sheets. The defects and un-ordered structures derived from GO are not recovered completely. When the reaction time is 12 h, some thinner and fasciolar graphene sheets tightly inlay on the large tracts of graphene sheets (Fig. 5b), which is the typical structure of GA. With further increasing the time to 20 h, the cross linked porous structure and the average size of the graphene sheets is obviously smaller and adhered tightly. In addition, the GA prepared at this reaction time is crumbly and has a poor elasticity. When the reaction time prolongs to 24 h, GA cannot be formed and is damaged into powders. Fig. S4 shows the photographs of the GAs obtained at various reaction times. The optimized reaction time windows are 8-16 h if using ammonia as reducing agent. On the other hand, the GA reduced by EDA exhibited an absolutely different behaviour. There are no obvious discriminations of the GA

at different reaction times (Fig. 5d-f), which were also confirmed by the high magnification SEM images (Fig. S5). Hence, EDA reveals a wide reaction time window ranging from 4 to 24 h for the formation of GA. These results matched well with the subsequent adsorption capacity performances (Fig. 6).

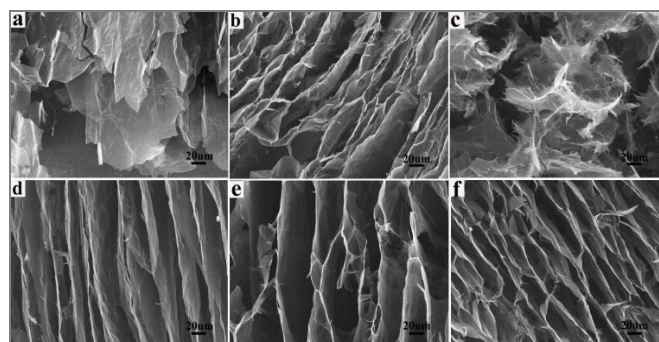


Fig. 5 SEM images of GA reduced with ammonia for (a) 4 h, (b) 12 h and (c) 20 h at 120 °C and SEM of GA reduced by EDA for (d) 4 h, (e) 12 h and (f) 20 h at 120 °C.

Both lube and n-hexane were used to evaluate the Q_{wt} of the samples reduced by different agents with various times. When ammonia and VC are used as reducing agents, the Q_{wt} for both lube and n-hexane are greatly reduced with prolonging the reaction time (Fig. 6). Nevertheless, the adsorption performances of the GA reduced with EDA is relatively stable compared to the other GAs. These results are consistent with the SEM observations (Fig. 5). The GA reduced by ammonia is destroyed into slag when the reaction time reaches of 24 h and thus no Q_{wt} was indicated in Fig. 6. These results reveal that prolonging the reaction time could destroy the 3D structure of GA. In general, increasing the time of hydrothermal reaction is of benefit to the reduction process of the GO and could promote the formation of π - π conjugated bond among graphene sheets, which can significantly affect the morphology and adsorption performance. Among the studied reducing agents, only EDA is insensitive to the reaction time and the obtained GA reveals a stable morphology and adsorption performances (Fig. 5 and Fig. 6).

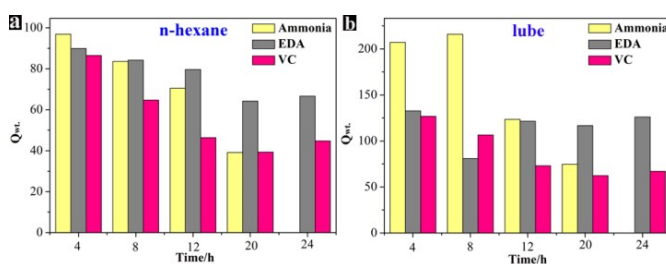


Fig. 6 The adsorption capacity for (a) n-hexane and (b) lube of the GAs prepared by different reducing agents at 120 °C for different reaction times.

3.3 The effects of reaction temperature

During the synthesis process, it was found that the hydrothermal temperature has notable influences on the appearance and volume of GA. Therefore, the reaction time is fixed at 6 h and the role of temperature on the morphology and adsorption performance is

further studied. The investigated temperature range is between 80 and 180 °C on the basis of the previous work.^{8,15} The hydrogel of GA cannot be formed when the temperature is below 80 °C, whereas the 3D structure of GA could be destroyed when temperature is above 180 °C. The SEM images of the GAs reduced by ammonia and EDA at different temperatures are shown in Fig. 7. With increasing the reaction temperature, graphene sheets transform from smooth layers to roughness, which was marked as red rings in Fig. 7. This is impressive since the conventional graphene sheets are very smooth (Fig. 7a and 7d). The results are further confirmed by the low magnification SEM images as well (Fig. S6 and S7). When the temperature is below 120 °C and ammonia is used as reducing agent, the hydrogel cannot be formed from the GO suspension no matter how long the reaction time is. In addition, the size of hydrogel decreased severely once the temperature is higher than 180 °C. In comparison with ammonia, EDA exhibits a wider temperature window and the GA can be obtained from 100 to 180 °C. Previous work has demonstrated that even in the absence of reducing agents, the hydrothermal treatment at appropriate time and temperature can promote the graphene sheets to reduce from the GO dispersion and can recover most of the destroyed structure.⁶ The addition of reducing agents can significantly accelerate this process. Generally, the demands for the temperature could vary with the different reducing agents. VC exhibits the widest temperature window among the studied reducing agents. Nevertheless, the high temperature can destroy the π -conjugated structures of the graphene sheets, which generate some small fragments on the graphene sheets as shown in Fig. 7.

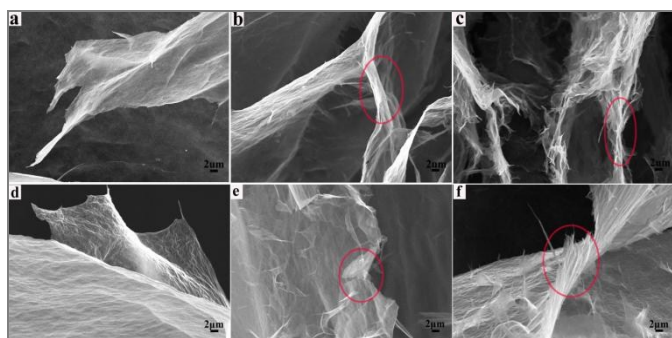


Fig. 7 SEM images of GA reduced with ammonia at (a) 120 °C, (b) 150 °C and (c) 180 °C for 6 h and of GA reduced by EDA at (d) 120 °C, (e) 150 °C and (f) 180 °C for 6 h.

The influences of reaction temperature on the adsorption performances were studied and shown in Fig. 8. As discussed above, the GA fabricated with VC possesses the widest range of reduction temperature ranging from 80 to 180 °C. The macroscopic size of the prepared GA decreases sharply within the initial 80 to 100 °C and subsequently keep almost unchanged. The size decreasing is also reflected from the adsorption capacity of the GAs, which causes the reduction of the adsorption performances. Using EDA as reducing agent seems to follow the same trend as the VC. From 100 to 140 °C, the sizes of the prepared GA shrink obviously and little changes have been indicated subsequently. The adsorption for both n-hexane and lube decreased evidently at the temperature range of 100 to 140 °C and stabilized subsequently, which is in accordance with the transformation of macroscopic appearance. The adsorption of the GAs reduced by ammonia and EDA at 80 °C was

not indicated in Fig. 8 due to the difficulty for the formation of hydrogel at these conditions. Compared to VC and EDA, the Q_{wt} of the sample reduced by ammonia is even more sensitive to temperature and has the narrowest window among the studied reducing agents.

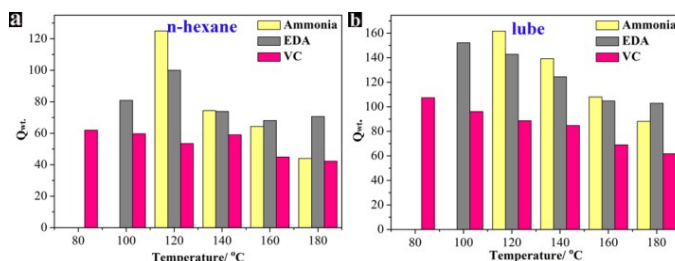


Fig. 8 The adsorption capacity for (a) n-hexane and (b) lube of the GAs prepared by different reducing agents for 6 h with different temperature.

4. Conclusions

In summary, we have systematically studied the effects of various reducing agents and hydrothermal conditions on the density, strength, morphology and adsorption performance of graphene aerogels. The graphene aerogel reduced by ammonia possesses the lowest density (4.9 mg/cm^3) and the highest specific surface area ($1089 \text{ m}^2/\text{g}$). Hence, this sample exhibits the highest adsorption capacity (Q_{wt}) for both lube (160 g g^{-1}) and n-hexane (105 g g^{-1}), but reveals the worst mechanical strength which leads to a sharp decreasing of Q_{wt} during adsorption-squeezing experiments. Furthermore, the graphene aerogel obtained with ammonia is very sensitive to the reaction time and temperature compared to other reducing agents. Although the graphene aerogel reduced by vitamin C performed the best hydrophobicity, the adsorption capacity is unsatisfactory. Take into consideration various factors, ethanediamine is a promising reducing agent for hydrothermal process because the obtained graphene aerogel cannot only maintain the high adsorption capacity but also reveal a wide hydrothermal preparation window. Our current work provides some hints to select reducing agent to prepare graphene aerogel for oil sorption.

Acknowledgements

We thank financial support by the Sichuan Youth Science and Technology Foundation (2013JQ0034), the Technology Foundation for Selected Overseas Chinese Scholar, Ministry of Personal, the Innovative Research Team of Sichuan Province and SWPU (2016TD0011, 2012XJZT002). We thank Dr. Hao Liu at Chengdu Green Energy and Green Manufacturing Technology R&D Center for Raman spectra measurements.

Notes and references

^aState Key Laboratory of Oil and Gas Reservoir Geology and Exploitation, Southwest Petroleum University, Chengdu 610500, China.

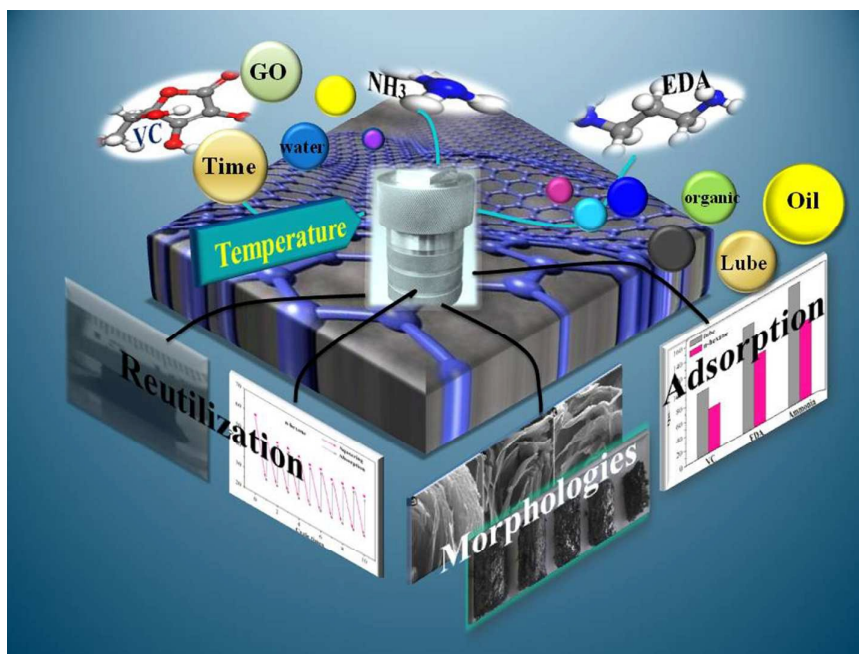
E-mail: yzhou@swpu.edu.cn

^bThe Center of New Energy Materials and Technology, School of Materials Science and Engineering, Southwest Petroleum University, Chengdu 610500, China

† Electronic Supplementary Information (ESI) available: [Fig. S1-S7, Table S1-S2] see DOI:

- 1 (a) M. Toyoda and M. Inagaki, *Spill Sci. Technol. Bull.* 2007, **8**, 467; (b) M. Schrope, *Nature*, 2011, **472**, 152-154.
- 2 (a) M. A. Worsley, P. J. Pauzauskie, T. Y. Olson, J. Biener, J. H. Satcher and Jr., T. F. Baumann, *J. Am. Chem. Soc.*, 2010, **132**, 14067-14069; (b) Y. Y. Fan, W. G. Ma, D. X. Han, S. Y. Gan, X. D. Dong and L. Niu, *Adv. Mater.* 2015, **27**, 3767-3773.
- 3 X. C. Dong, J. Chen, Y. W. Ma, J. Wang, M. B. Chan-Park, X. Liu, L. H. Wang, W. Huang and P. Chen, *Chem. Commun.*, 2012, **48**, 10660-10662; (b) X. C. Gui, Z. P. Zeng, Z. Q. Lin, Q. M. Gan, R. Xiang, Y. Zhu, A. Y. Cao and Z. K. Tang, *ACS Appl. Mater. Interfaces*, 2013, **5**, 5845-5850.
- 4 (a) R. J. White, N. Brun, V. L. Budarin, J. H. Clark and M. M. Titirici, *ChemSusChem*, 2014, **7**, 670-689. (b) Z. Y. Wu, C. Li, H. W. Liang, J. F. Chen, S. H. Yu, *Angew. Chem. Int. Ed.* 2013, **125**, 2997-3001.
- 5 (a) Y. Zhou, Q. L. Bao, L. A. Ling Tang, Y. L. Zhong and K. P. Loh, *Chem. Mater.*, 2009, **21**, 2950-2956; (b) S. Nardecchia, D. Carriazo, M. L. Ferrer, M. C. Gutierrez and F. del Monte, *Chem. Soc. Rev.*, 2013, **42**, 794-830.
- 6 D. C. Marcano, D. V. Kosynkin, J. M. Berlin, A. Sinitskii, Z. Z. Sun, A. Slesarev, L. B. Alemany, W. Lu and J. M. Tour, *ACS Nano*, 2010, **4**, 4806-4814.
- 7 Y. X. Xu, K. X. Sheng, C. Li, and G. Q. Shi, *ACS Nano*, 2010, **4**, 4324-4330.
- 8 (a) W. F. Chen, S. Li, C. H. Chen and L. F. Yan, *Adv. Mater.*, 2011, **23**, 5679-5683; (b) S. Stankovich, D.A. Dikin, R. D. Piner, K. A. Kohlhaas, A. Kleinhammes, Y. Y. Jia, Y. Wu, S. B. T. Nguyenb and R. S. Ruoffa, *Carbon*, 2007, **45**, 1558-1565; (c) D. Li, M. B. Müller, S. Gilje, R. B. Kaner and G. G. Wallace, *Nat. Nanotechnol.* 2008, **3**, 101-105; (d) H. J. Shin, K. K. Kim, A. Benayad, S. M. Yoon, H. K. Park, I. S. Jung, M. H. Jin, H. K. Jeong, J. M. Kim, J. Y. Choi and Y. H. Lee, *Adv. Funct. Mater.*, 2009, **19**, 1987-1992; (e) H. C. Bi, X. Xie, K. B. Yin, Y. L. Zhou, S. Wan, L. B. He, F. Xu, F. Banhart, L. Sun and R. S. Ruoff, *Adv. Funct. Mater.*, 2012, **22**, 4421-4425; (f) X. T. Zhang, Z. Y. Sui, B. Xu, S. F. Yue, Y. J. Luo, W. C. Zhan and B. Liu, *J. Mater. Chem.*, 2011, **21**, 6494-6497.
- 9 (a) H. Hu, Z. B. Zhao, W. B. Wan, Y. Gogotsi and J. H. Qiu, *Adv. Mater.*, 2013, **25**, 2219-2223; (b) J. H. Li, J. Y. Li, H. Meng, S. Y. Xie, B. W. Zhang, L. F. Li, H. J. Ma, J. Y. Zhang and M. Yu, *J. Mater. Chem. A*, 2014, **2**, 2934-2941.
- 10 (a) S. Kabiri, D. N. H. Tran, T. Altalhi and D. Losic, *Carbon*, 2014, **80**, 523-533; (b) B. C. Qiu, M. Y. Xing and J. L. Zhang, *J. Am. Chem. Soc.*, 2014, **136**, 5852-5855; (c) H. P. Cong, X. C. Ren, P. Wang and S. H. Yu, *ACS Nano.*, 2012, **6**, 2693-2703;
- 11 Z. Fan, D. Z. Y. Tng, C. X. T. Lim, P. Liu, S. T. Nguyen, P. F. Xiao, A. Marconnet, C. Y. H. Lim and H. M. Duong, *Colloids and Surfaces A: Physicochem. Eng. Aspects*, 2014, **445**, 48-53.
- 12 W. F. Chen and L. F. Yan, *Nanoscale*, 2011, **3**, 3132-3137.
- 13 W. C. Wan, R. Y. Zhang, W. Li, H. Liu, Y. H. Lin, L. N. Li and Y. Zhou, *Environ. Sci.: Nano*, 2016, DOI: 10.1039/c5en00125k.
- 14 Z. Xu, H. Y. Sun, X. L. Zhao and C. Gao, *Adv. Mater.*, 2013, **25**, 188-193.
- 15 (a) D. N. H. Tran, S. Kabiri, T. R. Sim and D. Losic, *Environ. Sci.: Water Res. Technol.*, 2015, **1**, 298-305. (b) M. Sun, Q. Tang, T. Zhang and G. Wang, *RSC Adv.*, 2014, **4**, 7774-7779; (c) C. Yang, J. Shen, C. Wang, H. Fei, H. Bao and G. Wang, *J. Mater. Chem. A.*, 2014, **2**, 1458-1464.
- 16 Z. Sui, Q. Meng, X. Zhang, R. Ma and B. Cao, *J. Mater. Chem.*, 2012, **22**, **18**, 8767-8771.
- 17 (a) L. M. Xu, G. Y. Xiao, C. B. Chen, R. Li, Y. Y. Mai, G. M. Sun, D. Y. Yan, *J. Mater. Chem. A*, 2015, **3**, 7498-7504. (b) H. C. Bi, K. B. Yin, X. Xie, Y. L. Zhou, N. Wan, F. Xu, F. Banhart, L. T. Sun and R. S. Ruoff, *Adv. Mater.*, 2012, **24**, 5124-5129.
- 18 (a) X. B. Fan, W. C. Peng, Y. Li, X. Y. Li, S. L. Wang, G. L. Zhang and F. B. Zhang, *Adv. Mater.* 2008, **20**, 4490-4493; (b) C. Bosch-Navarro, E. Coronado, C. Marti-Gastaldo, J. F. S

anchez-Royo and M. Gomez Gomez, *Nanoscale*, 2012, **4**, 3977-3982.



The different reducing agents including vitamin C, ammonia and ethanediamine can significantly affect the density, strength, morphology and adsorption performance of graphene aerogel.